

A 14% efficient nonaqueous semiconductor/liquid junction solar cell

James F. Gibbons,^{a)} George W. Cogan, Chris M. Gronet, and Nathan S. Lewis^{b)}
SERA Solar Corporation, Santa Clara, California 95054

(Received 20 July 1984; accepted for publication 21 August 1984)

We describe the most efficient semiconductor/liquid junction solar cell reported to date. Under W-halogen (ELH) illumination, the device is a 14% efficient two-electrode solar cell fabricated from an *n*-type silicon photoanode in contact with a nonaqueous electrolyte solution. The cell's central feature is an ultrathin electrolyte layer which simultaneously reduces losses which result from electrode polarization, electrolyte light absorption, and electrolyte resistance. The thin electrolyte layer also eliminates the need for forced convection of the redox couple and allows for precise control over the amount of water (and other electrolyte impurities) exposed to the semiconductor. After one month of continuous operation under ELH light at 100 mW/cm², which corresponds to the passage of over 70 000 C/cm², thin-layer cells retained over 90% of their efficiency. In addition, when made with Wacker Silso cast polycrystalline Si, cells yield an efficiency of 9.8% under simulated AM1 illumination. The thin-layer cells employ no external compensation yet surpass their corresponding experimental (three-electrode) predecessors in efficiency.

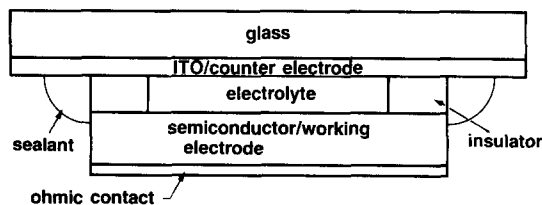
Much attention has been focused on semiconductor/liquid junction solar cells as an alternative to solid state devices.^{1,2} Liquid junction cells offer potential cost advantages over their solid-state counterparts. For example, the processing required to form a diffused junction in a solid-state device is replaced by the simple immersion of the semiconductor in a liquid. In 1978 Heller *et al.* reported the first highly efficient (12%) liquid junction solar cell.^{1a} Since then, Heller and others have shown that several materials can be stabilized in aqueous solvents while simultaneously achieving high efficiencies.^{1b} Another approach to limiting photo-corrosion has been to employ nonaqueous solvents,³⁻⁵ but until recently, efficiencies in these solvents were disappointingly low. Many of the early nonaqueous results were ascribed to the presence of electronic states at the semiconductor/liquid interface.⁶ However, from the current-voltage characteristics of experimental cells developed utilizing potentiostatic control, it was concluded that (1) in several systems, interface states were not limiting the cell efficiencies, and (2) that high efficiency junctions could be realized by drastically reducing the uncompensated cell resistance. Based on these ideas, studies of passivated systems have demonstrated that nonaqueous solvents can provide media where systematic design of highly efficient, nearly ideal semiconductor/liquid interfaces is possible.⁷⁻¹¹

Although efficient *aqueous* two-electrode cells have been demonstrated by Heller and others, the only efficient *nonaqueous* systems to date have been three-electrode cells which utilize external potentiostatic control and do not necessarily represent practical prototypes. Nonaqueous two-electrode cell design entails many difficulties including the following: limited stability of both forms of the redox couple, excessive absorption of light by the solution, low solubility of the redox pair, insufficient conductivity of the electrolyte, and the presence of trace amounts of corrosive water.^{12,13}

The thin-layer cell design, depicted in Fig. 1, simultaneously circumvents several of these difficulties. A liquid

electrolyte is sandwiched between a transparent glass cover, which is coated with a conducting indium-tin-oxide (ITO) film to serve as the counterelectrode. A thin electrical insulator isolates the two electrodes and maintains the desired interelectrode spacing. Incident light passes through the glass and the solution and impinges on the semiconductor surface. The device equations in Fig. 1 indicate that decreases in electrolyte thickness will improve all of the crucial design parameters of the systems.

Some of the potential advantages of a thin-layer cell design have been proposed previously,^{10,13,14} but cells which have been constructed have not been efficient.¹³ A key feature of our system is that the cell is sufficiently thin to effectively eliminate all of the losses which arise from the solution. Calculation of the relevant variables for typical cell parameters (Table I) reveals that, even in nonaqueous solvents, electrolyte losses can be minimized by using interelectrode spacings of 10–20 μm. The thin-layer cell design offers advantages even when compared to conventional three-electrode cells which employ an external power supply and electronic feedback to compensate for losses. Series resistance losses are much smaller than uncompensated resistance



Device equations:

$$J_L = \frac{2FD C_0}{t} \quad A = \epsilon t C_0 \quad V_d = J \rho t$$

FIG. 1. Cross section of a typical thin-layer liquid junction solar cell (not to scale), and the three equations which govern its operation. J_L is the diffusion-limited current density in an electrolyte layer of thickness t . F is Faraday's constant and D , C_0 , and ϵ are the diffusion coefficient, concentration, and molar extinction coefficient of the redox species, respectively. V_d is the ohmic voltage drop in the electrolyte, J is the cell current density, and ρ is the electrolyte resistivity.

^{a)} Also with Stanford Electronic Laboratory, Stanford, CA 94305.

^{b)} Also with Dept. of Chemistry, Stanford University, Stanford, CA 94305.

TABLE I. Parameters of two- and three-electrode cells: J_{sc} , V_{oc} , ff, and η are the short circuit current density, open circuit voltage, fill factor, and efficiency of the cell, respectively. t , A , J_L , and V_d are the thin-layer cell parameters as defined in Fig. 1. $N_{H_2O}/N_{monolayer}$ is the ratio of the number of water molecules present in thin electrolyte to the number required to form a monolayer of oxide (assuming a monolayer of oxide contains 5×10^{-10} moles/cm²). For the thin-layer cells the electrolyte was 0.15–0.2 M 1, 1'-dimethylferrocene/0.15–0.2 M 1, 1'-dimethylferricenium tetrakis(pentafluorophenyl)borate/1.0 M lithium perchlorate/methanol. For the three-electrode cells, the oxidized form of the redox pair was present at 0.5 mM, the electrolyte was magnetically stirred, and a Luggin capillary probe with a 0.2-mm outer diameter was used to limit the uncompensated ohmic resistance to approximately 50 Ω . In all cases illumination was provided by an ELH-type W-halogen solar simulator calibrated with a Solarex silicon secondary standard. Measurements made in natural sunlight agreed with those reported to within 5%.

	Characteristics of thin-layer and three electrode liquid junction cells				
	Single crystal silicon	Single crystal silicon ^a	Polycrystalline silicon	Single crystal silicon	Polycrystalline silicon
Type/dopant/resistivity (Ω cm)	<i>n</i> /phos/0.3	<i>n</i> /phos/0.3	<i>n</i> /phos/1–5	<i>n</i> /phos/4–9	<i>n</i> /phos/1.5
Surface	matte	matte	shiny	matte	shiny
Area (cm ²)	0.25	4.0	0.25	0.16	0.16
Configuration	thin layer	thin layer	thin layer	three electrode	three electrode
Illumination intensity (mW/cm ²)	100	100	100	70	70
J_{sc} (mA/cm ²)	34.0	28.0	27.4	25.0	18.0
V_{oc} (V)	0.60	0.61	0.53	0.53	0.53
ff	0.69	0.77	0.66	0.54	0.53
η (%)	14.0	13.1	9.6	10.1	7.2
t (μ m)	10 ± 5	15 ± 5	15 ± 5		
$N_{H_2O}/N_{monolayer}$ SiO ₂	< 3	< 3	< 3		
A (at 660 nm)	~0.07	~0.08	~0.08		
J_L (mA/cm ²)	> 75	> 60	> 60		
V_d (ohmic) (mV)	< 1	< 1	< 1		

^aNo corrections for 10% gold grid coverage.

losses present in a conventional three-electrode cell, even when the uncompensated resistance is minimized with the use of a Luggin capillary reference electrode. Concentration polarization losses due to the absence of high concentrations of both forms of the redox couple at the working and counterelectrodes are also minimized. Furthermore, in hermetically sealed thin-layer cells, standard laboratory techniques are sufficient to reduce the amount of water in the electrolyte such that prolonged corrosion processes may be eliminated.

We have demonstrated the fabrication of thin-layer devices using *n*-type silicon anodes in contact with the 1,1'-dimethylferrocene^{+ /0}/ methanol system. Techniques for formation of matte-etched *n*-type Si anodes are as described previously,¹⁰ except that an oxide gasket is formed around the device edges using photolithographic techniques. At present, the counterelectrode is a 5–20- Ω / \square resistivity indium-tin-oxide (ITO) (OCLI, Inc., Santa Rosa, CA); thus, samples larger than ~ 1 cm² require the addition of a gold grid on the ITO to increase its conductivity. The silicon and counterelectrode assembly is then clamped together and sealed with epoxy resin (Hysol Corp., Seabrook, NH). Finally, the solution is introduced through syringe needles attached to small holes in the ITO-coated glass. Typical cell thicknesses are 5–20 μ m (vide infra).

Figure 2 depicts the cell parameters of the *n*-Si/1,1'-dimethylferrocene^{+ /0}/ methanol system. Under 100 mW/

cm² of W-halogen (ELH) irradiation at room temperature, we observe open circuit voltages of 0.60–0.61 V, short circuit photocurrent densities of 28–34 mA/cm², fill factors of 0.69–0.77, and efficiencies of 14.0% \pm 1.0%. Short circuit current measurements in the sun and in the simulator were compared to establish the spectral similarities of the two sources. When normalized (Solarex silicon secondary reference) to Air Mass 1, the solar and simulator short circuit currents were 30.9 and 31.9 mA/cm², respectively. Thus the results agree to well within 5%. The open circuit voltage of these cells is higher than reported previously,¹⁰ due to a combination of higher current densities and optimization of bulk dopant densities and carrier lifetimes. The improved fill factors reflect the advantages of the thin-layer device design over conventional experimental cells (even under referenced potentiostatic control) in ohmic and concentration polarization losses.

Several single crystal *n*-Si/ propylene carbonate cells have been constructed to measure stability, and after one month of continuous operation at the maximum power point (> 70 000 C/cm² of charge) at 100 mW/cm² of ELH irradiation, a typical cell retained over 90% of its initial efficiency. Stability tests were terminated in each case because of seal failure, but no evidence of electrolyte or redox couple degradation was observed after this period. Solutions were dried using molecular sieves to initially contain less than 5 ppm of

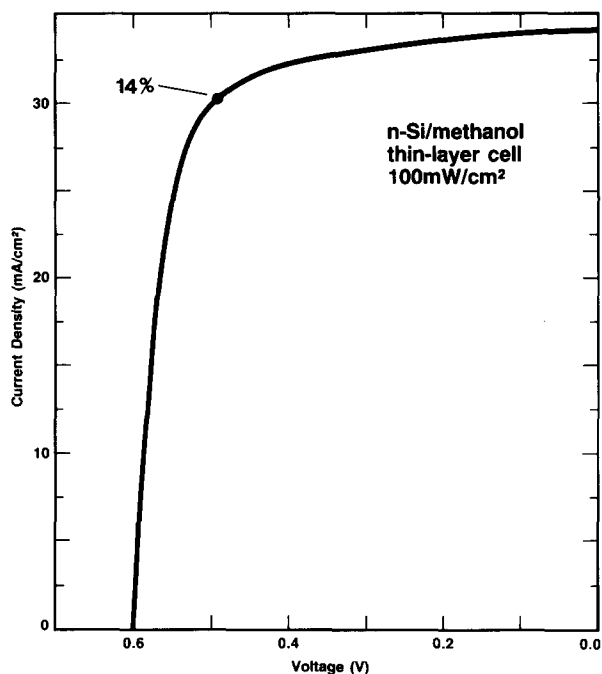


FIG. 2. Current-voltage characteristic of *n*-type single crystal Si thin-layer liquid junction solar cell. The solution is 0.15 *M* 1,1'-dimethylferrocene/0.15 *M* 1,1'-dimethylferricenium tetrafluoroborate/1.0 *M* lithium perchlorate/methanol (dried with 3 Å Linde molecular sieves). Incident light is 100 mW/cm² from an ELH-type W-halogen solar simulator. Cell conversion efficiency is 14%. See Table I, column 1, for more details.

water as measured by Karl Fischer titration. In a conventional Si/propylene carbonate cell, much lower water concentrations would be required to achieve long term stability. Since the thin-layer cell has such a high surface area to volume ratio, the total number of water and oxygen molecules present in the electrolyte can be less than the number required to cause deleterious effects.

The spectral response, versus incident photon wavelength for a typical *n*-Si/methanol cell shows external quantum yields which are greater than 0.8 for most of the visible portion of the spectrum (1.4–2.8 eV). The cell thickness has been estimated by measurement of the small decline in response at 660 nm due to the ferricenium ion ($\epsilon = 332 \text{ M}^{-1} \text{ cm}^{-1}$ at 660 nm for 1,1'-dimethylferricenium). The short wavelength response of the semiconductor/liquid junction cell is superior to that of conventional diffused *p-n* junction cells,¹⁵ indicating the absence of surface recombination sites or of surface "dead layers" which would decrease the photocurrent at short wavelengths. The 34-mA/cm² photocurrent density is within 20% of the 43-mA/cm² theoretically available from a Si absorber¹⁵; most of the remaining losses can be ascribed to optical absorption and reflection. Through judicious use of antireflection coatings, thinner solutions, and less colored redox couples, AMI cell efficiencies in the range of 16% could be obtained with the thin-layer silicon system.

We have also fabricated solar cells based upon Wacker cast polycrystalline Si substrates. The grains in this material are typically of 100–500- μm linear dimension with a preferred orientation of $\langle 100 \rangle$. As has been demonstrated previously,^{1,16} the intimate contact between the semiconductor and liquid can allow effective utilization of polycrystalline materials. As displayed in Table I, use of cast polycrystalline Si photoanodes yields a cell with an open circuit voltage of 0.53 V and efficiency of 9.6% under simulated AMI irradiation conditions. The remaining efficiency limitations on this cell are due to residual activity at grain boundary recombination sites.^{1,15,16} Again, when compared to previous three-electrode measurements,¹⁶ the thin-layer configuration yields improved cell behavior.

The results above indicate that nonaqueous semiconductor/liquid junction cells may provide an alternative to current photovoltaic energy conversion technologies. We demonstrate that application of insight gain from a three-electrode cell to an operating solar cell device can be accompanied by significant gains in both efficiency and stability. We also demonstrate that the thin-layer design is a compact, convenient scheme for fabrication of efficient semiconductor/liquid junction devices from some selected systems. Key remaining issues concerning long term stability, use of amorphous silicon substrates, and passivation of grain boundaries are under investigation.

We thank F. C. Wu, G. R. Model, L. A. Christel, J. T. Merchant, J. S. Olson, and R. Redse of SERA Solar Corp. and C. M. Lieber of Stanford University for valuable contributions to this work.

- ¹(a) A. Heller, B. A. Parkinson, and B. Miller, *Appl. Phys. Lett.* **33**, 512 (1978); (b) A. Heller, *Acc. Chem. Res.* **12**, 154 (1981); (c) D. Cahen, G. Hodes, J. Manassen, and R. Tenne, *ACS Symposium Ser.* **146**, 369 (1981).
- ²(a) T. M. Maugh, *Science* **221**, 1358 (1983); (b) S. Dennison, *Nature* **307**, 501 (1984).
- ³A. J. Bard and M. S. Wrighton, *J. Electrochem. Soc.* **124**, 1706 (1977).
- ⁴K. D. Legg, A. B. Ellis, J. M. Bolts, and M. S. Wrighton, *Proc. Natl. Acad. Sci.* **74**, 4116 (1977).
- ⁵S. N. Frank and A. J. Bard, *J. Amer. Chem. Soc.* **97**, 7427 (1975).
- ⁶A. J. Bard, A. B. Bocarsly, F.-R. F. Fan, E. G. Walton, and M. S. Wrighton, *J. Am. Chem. Soc.* **102**, 3671 (1980).
- ⁷C. M. Gronet and N. S. Lewis, *Nature* **300**, 733 (1983).
- ⁸C. M. Lieber, C. M. Gronet, and N. S. Lewis, *Nature* **307**, 533 (1984).
- ⁹C. M. Gronet and N. S. Lewis, *Appl. Phys. Lett.* **43**, 115 (1983).
- ¹⁰C. M. Gronet, N. S. Lewis, G. Cogan, and J. F. Gibbons, *Proc. Natl. Acad. Sci.* **80**, 1152 (1983).
- ¹¹N. S. Lewis, *Ann. Rev. Mat. Sci.* **14**, 95 (1984).
- ¹²P. A. Kohl and A. J. Bard, *J. Electrochem. Soc.* **126**, 603 (1979).
- ¹³M. E. Langmuir, P. Hoenig, and R. D. Rauh, *J. Electrochem. Soc.* **128**, 2357 (1981).
- ¹⁴B. A. Parkinson, *Solar Cells* **6**, 177 (1982).
- ¹⁵S. J. Fonash, *Solar Cell Device Physics* (Academic, New York, 1981), pp. 71 and 110.
- ¹⁶G. Cogan, C. M. Gronet, J. F. Gibbons, and N. S. Lewis, *Appl. Phys. Lett.* **44**, 539 (1984).